Malaysian Journal of Chemistry, 2016, Vol. 18(1), 60–68

Study on Hydrolysis of Poly(Lactic Acid)/Chitosan/Polyethylene Glycol Nanocomposites in Phosphate Buffer Solution

Nguyen Thi Thu Trang*, Nguyễn Thuy Chinh and Thai Hoang

Institute for Tropical Technology, Vietnam Academy of Sciece and Technology,
18 Hoang Quoc Viet, Cau Giay, Ha Noi

*Corresponding author (e-mail: trangvktnd@gmail.com)

Poly(lactic acid)/chitosan/polyethylene glycol (PLA/CS/PEG) nanocomposites were prepared by solution method. The content of PEG was 2 – 10 wt. % compared with the weight of PLA. The characterization and morphology of the nanocomposites before and after hydrolysis in phosphate buffer solution were determined by fourier transform infrared spectroscopy (FTIR), differential scanning calorimetry and scanning electron microscopy (SEM). The hydrolysis of PLA/CS/PEG nanocomposites in phosphate buffer solution for different testing time was also investigated. It was clear that the shift of wavenumber for C=O, OH, CH_3 groups in FTIR spectra of PLA/CS/PEG nanocomposites before and after hydrolysis. The SEM images of the PLA/CS nanocomposite in the presence of PEG indicated that PEG played a role in the improvement of interaction and dispersion between CS and PLA phases, limitation of permeability of phosphate buffer solution into the structure of the nanocomposites. The obtained results of hydrolysis after 28 testing days showed that the PLA/CS/PEG6 nanocomposite (containing 6 wt. % of PEG) had the lowest weight loss with highest regression coefficient ($R^2 = 0.9933$) in the phosphate buffer solution.

Key words: Poly (lactic acid); chitosan; nanocomposite; hydrolysis; polyethylene glycol; weight loss

Received: October 2014; Accepted: April 2016

Chitosan (CS), derived through the deacetylation of chitin, has aroused great interest as a new functional biomaterial because of its excellent biological properties such as antimicrobial activity, non-toxicity, biodegradability and biocompatibility [1, 2].

Polylactic acid (PLA), biodegradable thermoplastic polymer, has atttracted many researchers due to their good properties such as good adhesion, superior transparency, high mechanical properties, biodegradability and biocompatibility [3]. However, the high crystallinity, strong hydrophobicity and especially the lack of bioactive functions of PLA matrix has often resulted in an uncontrollable biodegradation rate and an undesirable biological response to cells and/or tissues. Therefore, it is promising to combine the bioactive functions of CS with the good mechanical properties of PLA to generate a new kind of biohybrid materials [4]. The earlier reports showed that the compatibility between PLA and CS was limited because of the different structure and hydrophilic property [5–10]. In a previous paper, we investigated the effect of PEG on morphology, thermal property and hydrolysis of PLA/CS composites [10]. There are clear evidence for the interactions such as hydrogen bonds and dipole-dipole interactions between hydroxyl groups of PEG with amino, C-O-C, hydroxyl groups of the CS and carboxyl, C-O-C, hydroxyl groups of PLA in the composite. The results obtained clearly showed that PEG played an important role in increase the compatibility

between PLA and CS phases. In this study, we have focused to study on some properties and hydrolysis ability of PLA/CS nanocomposites using PEG before and after hydrolysis in phosphate buffer solution which is nearly similar to simulated body fluid.

EXPERIMENT

Materials

Poly (lactic acid) was purchased from NatureWorks LLC, USA. Chitosan and polyethylene glycol were obtained from Sigma-Aldrich, USA. Chloroform, phosphate buffer solution and acetic acid were analytical grades and used without further purification.

Preparation of PLA/CS Nanocomposites

Solution method was applied for preparation of PLA/CS nanocomposites. PLA (1.5 wt.%) was dissolved in chloroform to form a fine solution. CS (at a concentration of 20 wt.% in comparison with PLA weight) was dissolved in acetic acid 1% solution (v/v) at room temperature under magnetic stirring. PEG as a compatibilizer was added to the PLA solution at different content (0, 2, 4, 6, 8, 10 wt.% PEG compared with PLA) that were abbreviated as PLA/CS; PLA/CS/PEG2, PLA/CS/PEG4, PLA/CS/PEG6, PLA/CS/PEG8, and PLA/CS/PEG10, respectively. The PLA/CS composites were obtained by solvent casting on Petri dishes, kept at room temperature for 24 h to evaporate solvent and then were dried in a vacuum oven at 40^{o}C for 8 h.

Characterization

Fourier Transform Infrared (FT-IR) spectra were recorded from 400 to 4000 cm^{-1} on the films of PLA/CS composites using a Nexus FTIR spectrophotometer at room temperature.

Field emission scanning electron microscopy (FE-SEM) was carried out on S4800 SEM to evaluate the morphology of PLA/CS composites and the dispersion of CS in PLA matrix.

Differential scanning calorimetry (DSC) analysis of PLA/CS composites were performed on DTG-60H and DSC-60 analyzer under Argon invironment and in the temperature range from room temperature to 500°C with a heating rate of 10°C per min.

Determination of weight loss of the samples in phosphate buffer solution is based on the weight change after hydrolysis by the formular: $m = ((m_b-m_s)/mb).100\%$, in which m is weight loss of samples (%), m_b is initial sample weight (g), and m_s is loss weight of samples after hydrolysis (g).

RESULTS AND DISCUSSION

FTIR of PLA/CS/PEG Nanocomposites before and After Hydrolysis in Phosphate Buffer Solution

Figure 1 shows FTIR spectra of PLA/CS/PEG6 nanocomposite before and after 28 testing days in phosphate buffer solution. In spectrum of PLA/CS/PEG6 nanocomposite before teating, it was clear the broad band at 3431 cm^{-1} corresponded to the amine and hydroxyl groups; the peak at 2993 cm^{-1} could be attributed to –CH stretching; the absorption band at 1754 cm^{-1} was due to the carbonyl (C=O) stretching of the secondary amine and the bending vibrations of the N-H at 1449 cm^{-1}. Additionally, the bending vibrations of the CH_3, $–NH_2$ were observed at 1367 cm^{-1} and 1449 cm^{-1}, respectively.

The shift of wave number of the above groups could be observed for the PLA/CS/PEG6 nanocomposite after testing in comparison with the original sample. The wave number of OH group shifted from 3431 cm^{-1} to 3446 cm^{-1} withexpanded peak, NH_2 group shifted from 1449 cm^{-1} to 1455 cm^{-1} with more weakintensity. Similarly, C=O group vibration moves from 1754 cm^{-1} to 1758 cm^{-1}. It can be explained that PLA might be hydrolyzed in phosphate buffer solution to break the ester linkages. This had led to the short segments of PLA, and LA oligomers which were separated from the nanocomposite.

Hydrolysis of PLA/CS/PEG Nanocomposites in Phosphate Buffer Solution

The hydrolysis process of PLA/CS/PEG nanocomposite in phosphate buffer was mainly due to the hydrolysis of the PLA by the direct

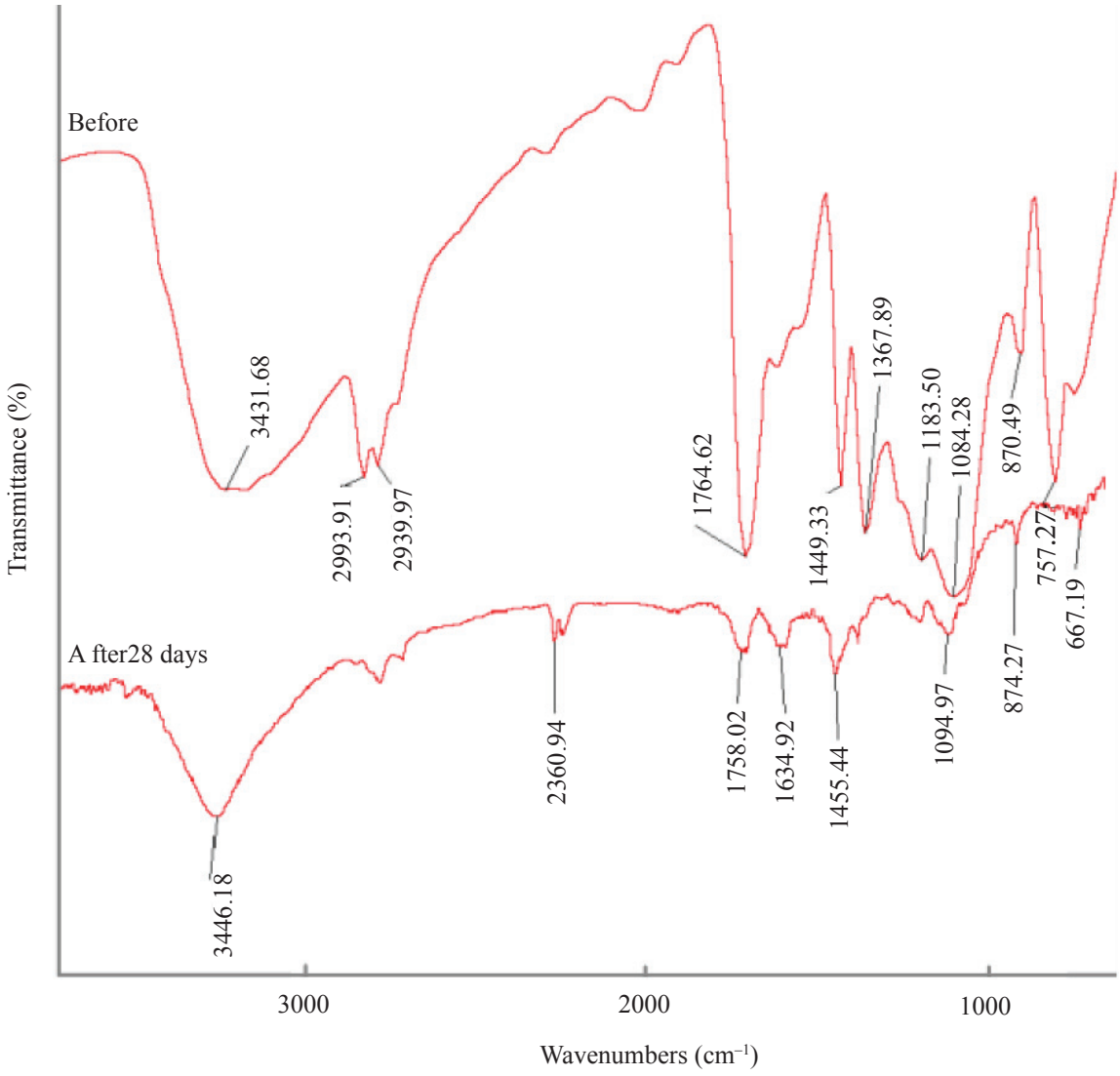

Figure 1. FTIR of PLA/CS/PEG6 nanocomposite before and after testing 28 days in phosphate buffer solution.

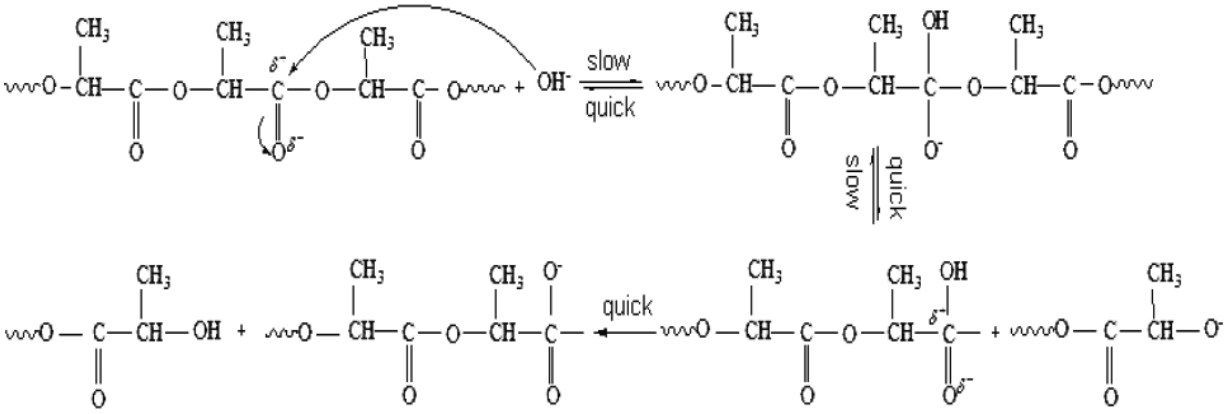

Figure 2. Hydrolysis mechanism of PLA in phosphate buffer solution (pH = 7.4).

influence of water and temperature. The hydrolysis mechanism of PLA in phosphate buffer (pH = 7.4) is shown in Figure 2 [11].

Figure 3 presents the loss of weight of PLA/CS/PEG nanocomposites versus testing time in the phosphate buffer of pH = 7.4.

Obviously, the weight loss of PLA/CS/PEG nanocomposites with different content of PEG was lower than that of PLA/CS nanocomposite after 2, 5, 7, 14, 28 days of hydrolysis in phosphate buffer solution. This could be explained by the presence of PEG which improved the dispersion and adhesion between CS and PLA phases and led to decrease numbers of defects and holes in the PLA/CS/PEG nanocomposites compared with PLA/CS nanocomposite. Thus, phosphate buffer solution was difficult to permeate into the PLA/CS/PEG nanocomposites and the hydrolysis of PLA

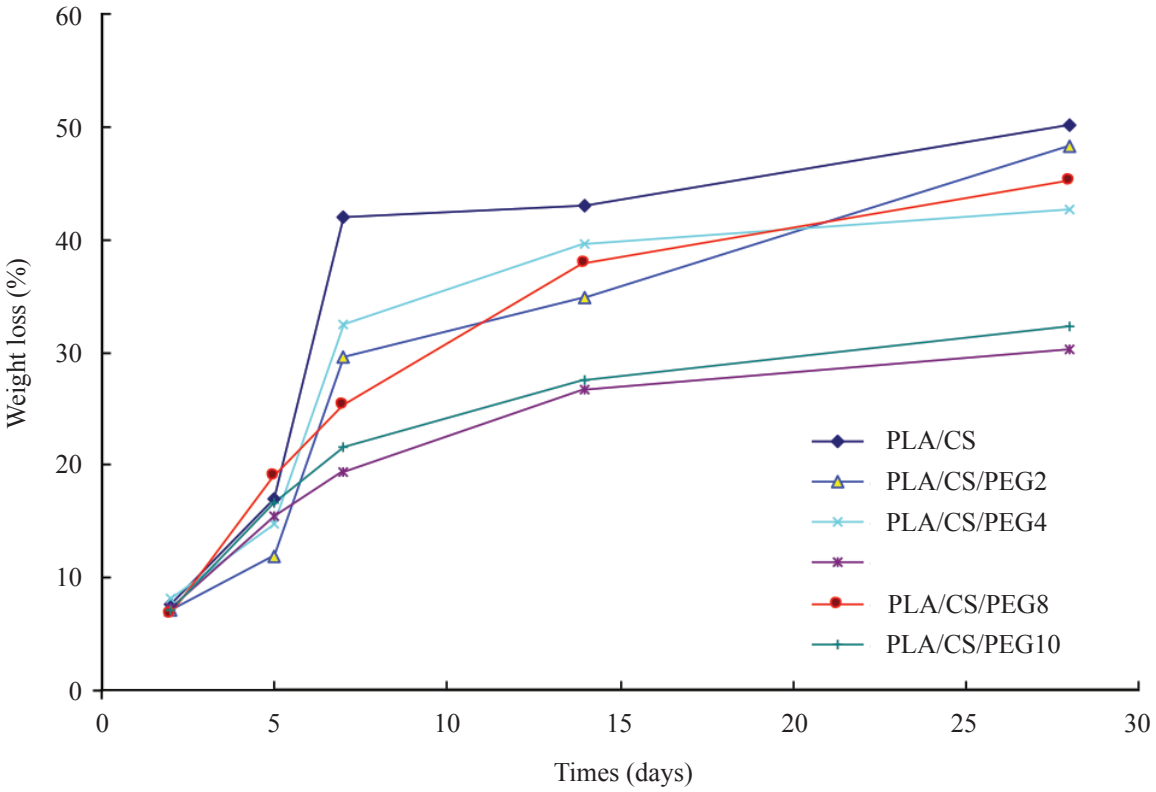

Figure 3. Weight loss of PLA/CS/PEG nanocomposites versus testing time in the phosphate buffer solution (pH = 7.4).

Table 2. The regression equation between the weight loss (Y-%) of the samples and the testing time (X-days) in phosphate buffer solution.

Sample	Regression equation	R^2
PLA/CS	$Y = -0.1205X^2 + 5.1427X - 0.1479$	0.8464
PLA/CS/PEG2	$Y = -0.0678X^2 + 3.5933X + 0.4141$	0.9272
PLA/CS/PEG4	$Y = -0.1057X^2 + 4.4873X - 0.3988$	0.9257
PLA/CS/PEG6	$Y = -0.083X^2 + 3.9099X + 0.6177$	0.9933
PLA/CS/PEG8	$Y = 8.9847Ln(X) + 1.4656$	0.9864
PLA/CS/PEG10	$Y = 9.6538Ln(X) + 1.3081$	0.9882

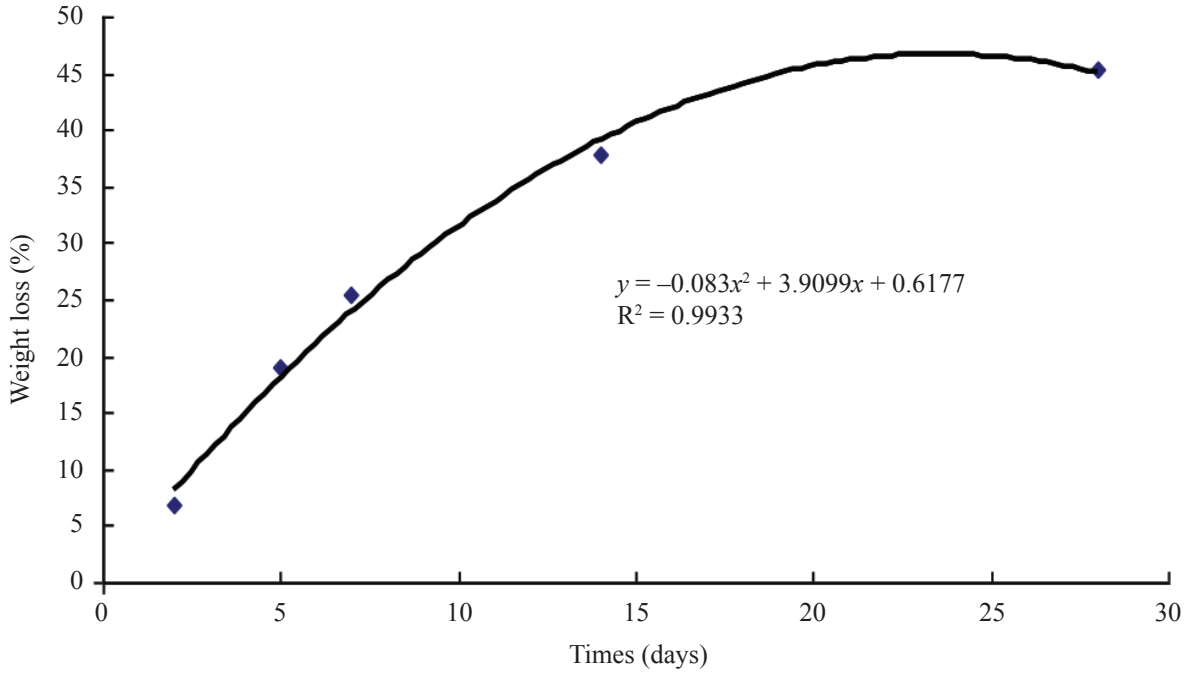

Figure 4. Weight loss of PLA/CS/PEG6 nanocomposites versus testing time in the phosphate buffer (pH =7.4).

in the nanocomposites was reduced. In the tested samples, the PLA/CS nanocomposite containing 8 wt.% of PEG had weight loss absolutely lower than the others for the same hydrolysis time in phosphate buffer solution.

According to the data obtained from Figure 3, the regression equations reflected the relationship between the weight loss of the samples and the testing time in phosphate buffer solutions is presented in Table 2.

It could be clearly seen from the Table 2 that all the equations obtained were suitable quadratic curves, with regression coefficients ranging from 0.8464 to 0.9933. The highest regression coefficient from the regression equations, reflected weight loss of PLA from PLA/CS/PEG6 nanocomposites hydrolyzed in phosphate buffer solution was 0.9933 and regression equations was $Y = -0.083X^2 + 3.9099X + 0.6177$ (Figure 4).

Morphology of PLA/CS/PEG Nanocomposites after Hydrolysis in Phosphate Buffer Solution

Structure of PLA/CS/PEG nanocomposite had an important influence on their hydrolysis process in different solutions. The tight structure of PLA/CS/PEG had more little hole and defects, resulted in limitation of permeability of phosphate buffer solution into structure of nanocomposites and PLA in nanocomposites was difficult to be hydrolyzed.

It could be clearly seen from the SEM images, the surface of the PLA/CS, PLA/CS/PEG4 and PLA/CS/PEG6 nanocomposites were destroyed after 28 testing days in the phosphat buffer solution (in Figure 5). In phosphate buffer solution, PLA/CS nanocomposite was hydrolyzed faster than PLA/CS/PEG nanocomposite although PLA phases in both nanocomposites were hydrolyzed to form the dark holes as seen in Figure 5. PEG enhances structure of PLA/CS nanocomposite by improving the compatibility between PLA and CS phases [10]. After hydrolysis, the number and size of holes and defects of PLA/CS nanocomposite (*PLA/CS.Buffer image*) are higher than those of PLA/CS/PEG nanocomposites (*PLA/CS/PEG4. Buffer and PLA/CS/PEG6.Buffer images*). The image of PLA/CS/PEG6 nanocomposite (6 wt.% of PEG) indicated the best compatibility between PLA and CS phases. This led to the fine and tight structure which would limit to the formation of holes and defects after hydrolysis of the samples in the phosphate buffer solution. The morphology

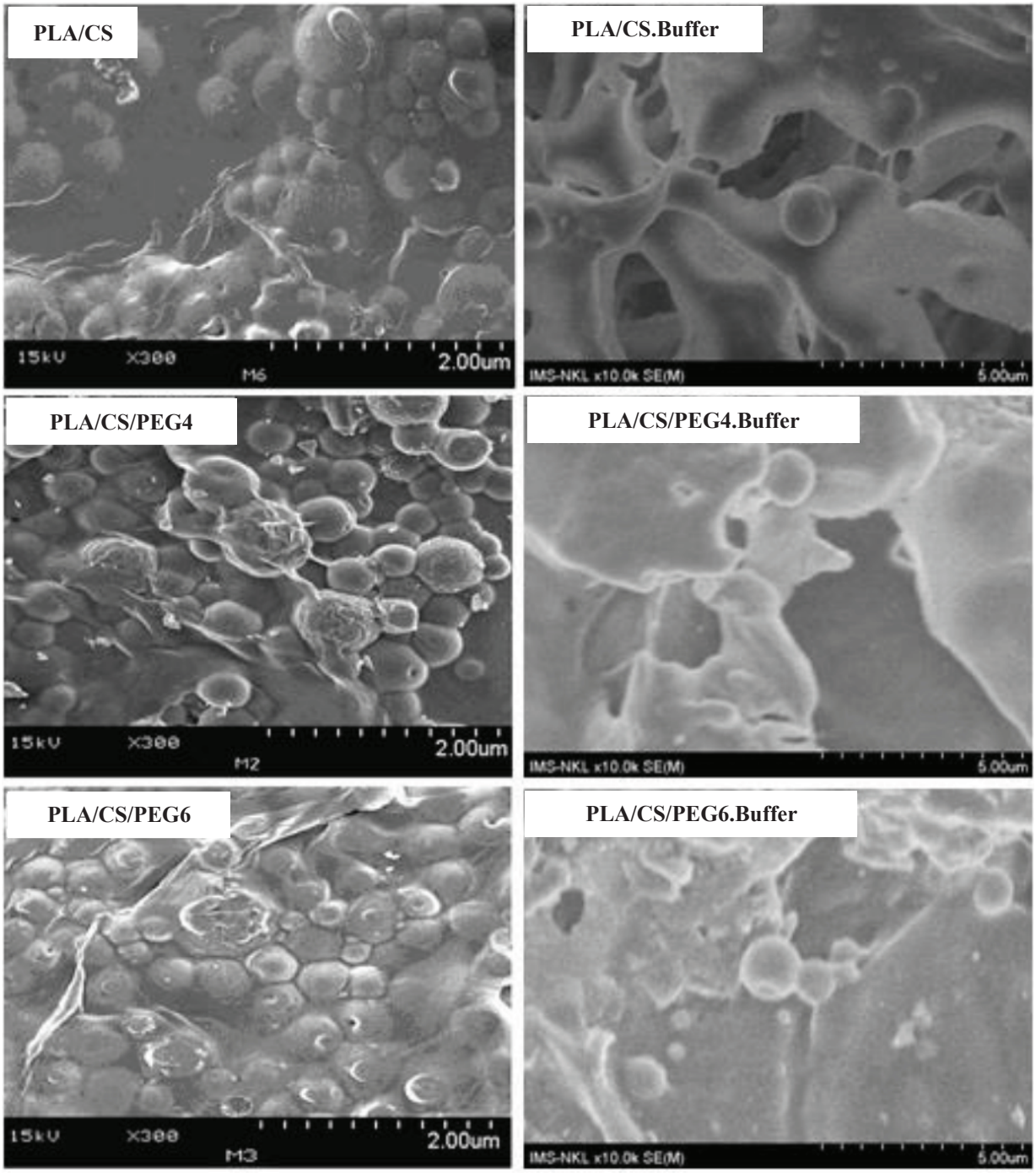

Figure 5. SEM images of PLA/CS, PLA/CS/PEG4, PLA/CS/PEG6 before and after 28 testing days in the phosphate buffer solution.

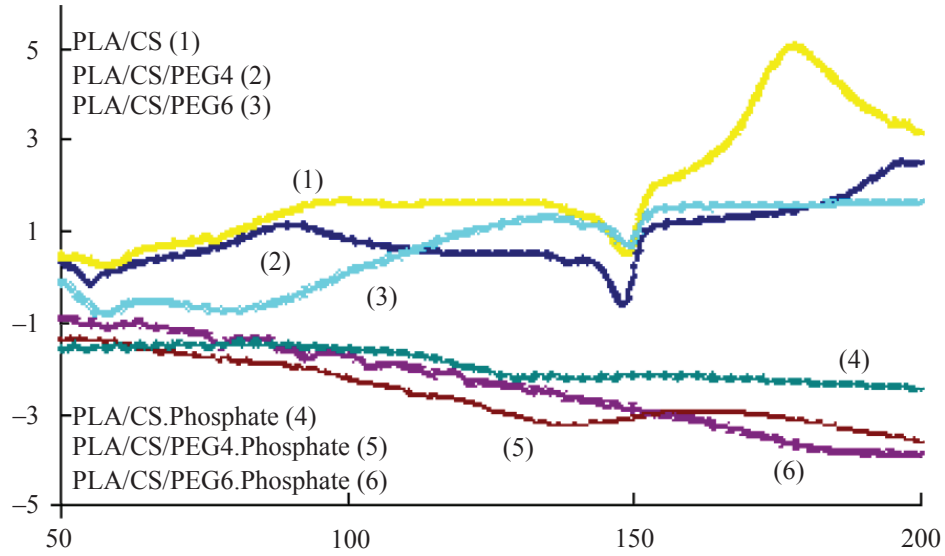

Figure 6. DSC thermograms of PLA/CS, PLA/CS/PEG4 and PLA/CS/PEG6 composites before and after 28 testing days in phosphate buffer solution.

Table 3. DSC data and the degree of crystallinity (χ_c) of PLA/CS/PEG nanocomposite before and after 28 testing days in phosphate buffer solution.

Sample	T_g (°C)		T_m(°C)		ΔH_m (J/g)		χ_c^* (%)	
	initial	28 days	initial	28 days	initial	28 days	initial	28 days
PLA/CS	54.7	61.9	149	152	10.6	18.17	11.4	19.44
PLA/CS/PEG4	54.0	64.2	150	154	11.4	22.52	12.2	24.19
PLA/CS/PEG6	59.6	63.6	151	157	16.4	29.84	17.7	32.05
PLA/CS/PEG8	56.2	62.5	151	155	15.8	28.51	16.9	30.62

*: χ_c (%) = ΔH_m x100/ΔH_m^* where ΔH_m^* is the heat of fusion for completely crystallized PLA (93.1 J/g) [8]. T_g: the glass transition temperature; T_m: the melting temperature; ΔH_c: the crystallization enthalpy; ΔH_m: the enthalpy of melting; χ_c: the degree of crystallinity.

of PLA/CS/PEG2, PLA/CS/PEG8 and PLA/CS/PEG10 nanocomposites were similar to the morphology of PLA/CS/PEG4.

Thermal Behaviour of PLA/CS/PEG Composite after Hydrolysis in Phosphate Buffer Solution

From the DSC curves of PLA/CS and PLA/CS/PEG nanocomposites before and after 28 testing days in phosphate buffer solution in Figure 6.

Thermal behaviours such as glass transition temperature (T_g), melting temperature (T_m), the enthalpy of melting (ΔH_m), the degree of crystallinity (χ_c) of the nanocomposites were calculated and listed in Table 3.

The T_g and melting temperature (T_m) of PLA/CS/PEG nanocomposites after hydrolysis were higher than those of original sample. T_g and T_m of PLA/CS nanocomposite with different content of PEG were higher than those of PLA/CS nanocomposite. This proves that using PEG, the PLA and CS phases are compatible because of hydrogen and dipole-dipole interactions [10]. The enthalpy of crystallization and melting of PLA/CS/PEG nanocomposites were higher than those of PLA/CS nanocomposite. This was due to the dispersion of CS into the PLA matrix was able to

lead to re-arrangement of the crystal structure of PLA. Especially, the physical interactions formed between the PEG, PLA and CS make crystal degree of PLA/CS/PEG6 and PLA/CS/PEG6 nanocomposites significantly increased.

After 28 testing days in phosphate buffer solution, the crystallinity of PLA/CS/PEG nanocomposites was higher than that of the nanocomposite before testing. This demonstrated the amorphous part of the PLA in the nanocomposites were hydrolyzed and the PLA crystal structure was re-arranged. Crystallinity of PLA/CS/PEG6 nanocomposite after hydrolysis in phosphate buffer solution was the highest.

CONCLUSION

FTIR analysis showed the shift of characteristic peaks on PLA/CS/PEG nanocomposites before and after testing in phosphate buffer solution. By using PEG in PLA/CS nanocomposites, the number of holes and defects in structure of the nanocomposites after hydrolysis were reduced as observed in FESEM images. After 28 testing days in phosphate buffer solution, the weight loss of PLA/CS/PEG nanocomposites was lower than that of PLA/CS nanocomposite. Among the tested samples, the weight loss of PLA/CS/PEG6 nanocomposite versus testing time was suitable to the regression equation $Y = –0.083X^2 + 3.9099X + 0.6177$ with maximum regress coefficient (R^2) of 0.9933. This sample had the highest crystallinity. The crystallinity of PLA/CS/PEG nanocomposite was higher than that of PLA/CS nanocomposite.

ACKNOWLEDGEMENTS

The authors would like to thank the National Foundation for Science and Technology Development for financial support in Vietnam (Subject code DT.NCCB-DHUD.2012-G/09, period of 2013 - 2016).

REFERENCES

1. Pillai, C. K. S., Paul, W. and Sharma, C. P. (2009) Chitin and chitosan polymers, *Progress in Polymer Science*, **34,** 1775–1792.
2. Jayakumar, R., Prabaharan, M., Sudheesh Kumar, P. T., Nair, S. V. and Tamura, H. (2011) Biomaterial based on chitin and chitosan in wound dressing application, *Biotechnology Advanced*, **29,** 322–337.
3. Nanda, R. Sasmal, A. and Nayak, P. L. (2011) Preparation and characterization of chitosan–polylactide composites blended with Cloisite 30B for control release of the anticancer drug Paclitaxel, *Carbohydrate Polymers*, **83**, 988–994.
4. Prabaharan, M. Rodriguez-Perez, M. A., de Saja, J. A. and Mano, J. F. (2007) Preparation and characterization of Poly(D,L-lactic acid)/chitosan Hybrid Scaffold with Drug Release Capability, *J. Biomed Mater Res B Appl Biomater*, **81**(2), 427–434.
5. Liao, Y. Z. Xin, M. H. Li, M. C. and Su, S. (2007) Preparation and characterization of O-lauroyl chitosan/polylactide blend membranes by solution-casting approach, *Chinese Chemical Letters*, **18**(2), 213–216.
6. Dev, A., Binulal, N. S., Anitha, A., Nair, S. V., Fruike, T., Tamura, H. and Jayakumar, R. (2010) Preparation of poly(lactic acid)/chitosan nanoparticles for anti-HIV drug delivery applications, *Carbohydrate Polymers*, **80**, 833–838.
7. Bonilla, J. Fortunati, E. Vargas, M., Chiralt, A. and Kenny, J. M. (2013) Effects of chitosan on the physicochemical and antimicrobial properties of PLA films, *Journal of Food Engineering*, **119(2)**, 236–243.
8. Jeevitha, D. and Amarnath, K (2013) Chitosan/PLA nanoparticles as a novel carrier for the delivery of anthraquinone: Synthesis, characterization and in vitro cytotoxicity evaluation, *Colloids and Surfaces B: Biointerfaces*, **101**, 126– 134.
9. Rajan, M. and Raj, V. (2013) Formation and characterization of chitosan-polylacticacid-polyethylene glycol-gelatin nanoparticles: A novel biosystem for controlled drug delivery, *Carbohydrate Polymers*, **98(1)**, 951–958.
10. Thai Hoang, Nguyen Thi Thu Trang, Nguyen Thuy Chinh, (2012) *Vietnam Journal of Chemistry*, **50(5)**, 570.
11. Araque-Monrós, M. C., Vidaurre, A., Gil-Santos, L., Bernabé, S. G., Monleón-Pradas, M. and Más-Estellés, J. (2013) Study on the degradation of new PLA braided biomaterial in buffer phssphate saline, basic and acid media, intended for the regeneration of tendons and ligaments, *Polymer Degradation and Stability*, **98**, 1563–1570.